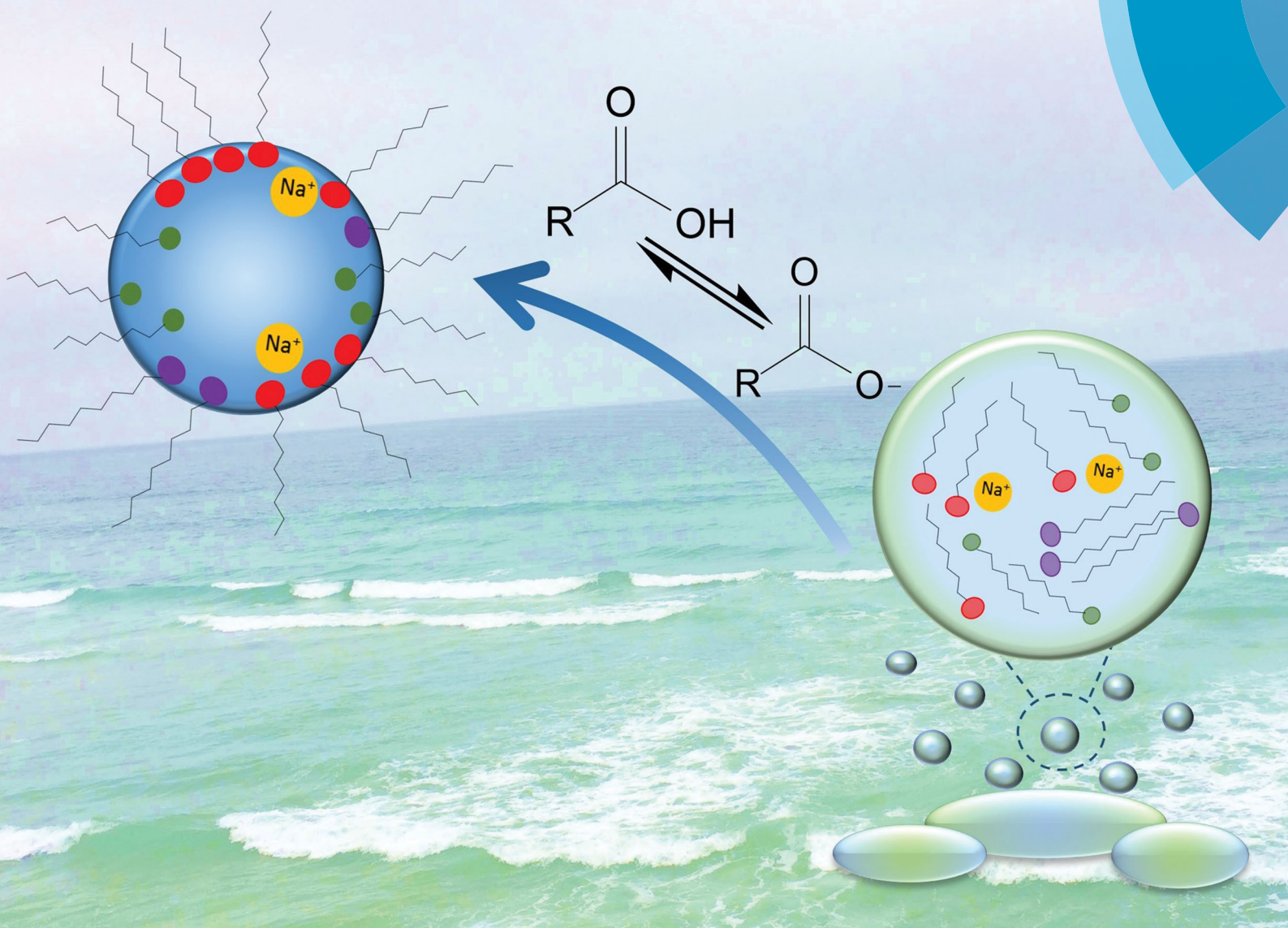


PCCP

Physical Chemistry Chemical Physics
rsc.li/pccp



ISSN 1463-9076



PAPER

Heather C. Allen *et al.*

Surface pK_a of octanoic, nonanoic, and decanoic fatty acids at the air-water interface: applications to atmospheric aerosol chemistry



Cite this: *Phys. Chem. Chem. Phys.*,
2017, 19, 26551

Surface pK_a of octanoic, nonanoic, and decanoic fatty acids at the air–water interface: applications to atmospheric aerosol chemistry†

Bethany A. Wellen, Evan A. Lach and Heather C. Allen *

There exists large uncertainty in the literature as to the pK_a of medium-chain fatty acids at the air–water interface. *Via* surface tension titration, the surface- pK_a values of octanoic (C_8), nonanoic (C_9), and decanoic (C_{10}) fatty acids are determined to be 4.9, 5.8, and 6.4, respectively. The surface- pK_a determined with surface tension differs from the bulk value obtained during a standard acid–base titration. Near the surface- pK_a of the C_8 and C_9 systems, surface tension minima are observed and are attributed to the formation of surface-active acid–soap complexes. The direction of the titration is shown to affect the surface- pK_a of the C_9 system, as the value shifts to 5.2 with NaOH titrant due to a higher concentration of Na^+ ions at pH values close to the surface- pK_a . As the reactivity and climate-relevant properties of sea spray aerosols (SSA) are partially dictated by the charge and surface activity of the organics at the aerosol–atmosphere interface, the results presented here on SSA-identified C_8 – C_{10} fatty acids can be used to better predict the health and climate impact of particles with significant concentrations of medium-chain fatty acids.

Received 5th July 2017,
Accepted 8th August 2017

DOI: 10.1039/c7cp04527a

rsc.li/pccp

Introduction

The air–water interface provides a unique environment for chemistry due to its asymmetry and 2-D intermolecular interactions.^{1,2} As the local environment at the interface is different from the bulk, one would expect the pK_a (an expression of acidity) of surface-active molecules to deviate from bulk values. This deviation can be attributed to increased interactions between molecular groups as a result of van der Waals forces between longer hydrocarbon chains,³ a change in the local pH at the surface due to the charge density of the surface film,^{4–6} or a change in the effective dielectric constant of the medium surrounding the headgroups of molecules at the interface.^{7–10}

Fatty acids constitute a common class of surface-active molecules which are studied at the air–water interface. Some studies have shown that as the hydrophobic chain length of the acid increases, and the molecules become more surface active, the pK_a also increases.^{3,11} However, it has been commonly, and incorrectly, reported in literature that the pK_a of medium-chain

fatty acids (C_8 – C_{10}) at the interface is the same as that of their bulk counterpart.^{12–14} As the surface- pK_a of these medium-chain fatty acids seem ill-defined, one might be inclined to examine the trends of other physical properties (solubility and critical micelle concentration (CMC)) against carbon chain length for these saturated compounds (Fig. 1).^{15,16} Between two and six carbons, the acids are very soluble (from ∞ to 0.97 g/100 g H_2O) and have higher CMC values (indicating that

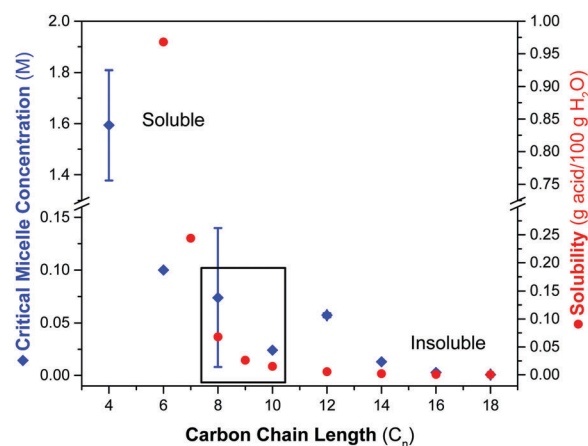


Fig. 1 Trends of CMC (blue diamonds)¹⁶ and solubility (red circles)¹⁵ with carbon chain length of saturated fatty acids. C_8 – C_{10} fatty acids fall between the soluble and insoluble groups of this molecular class.

Department of Chemistry & Biochemistry, The Ohio State University, Columbus, Ohio 43210, USA. E-mail: allen@chemistry.ohio-state.edu

† Electronic supplementary information (ESI) available: This material includes (1, 2) adsorption isotherms of nonanoic acid at pH 2 and pH 12, (3) weak acid–strong base bulk titration of 1 mM nonanoic acid, (4) derivation of the surface activity model bounds, (5) IRRAS spectra comparing the CH stretching modes of a stearic acid Langmuir monolayer to a 1 mM nonanoic acid Gibbs monolayer, (6) surface tension titration of acetic acid as a control study. See DOI: 10.1039/c7cp04527a

a large concentration is necessary for the required molecular associations to form micelles). For acids with chain lengths of twelve or more carbon atoms, solubility and CMC remain relatively constant at low values. Between these two regimes lies the class of medium-chain fatty acids, which are on the cusp of being considered in the same context as their insoluble, surface-active ($C_n \geq 12$) counterparts as opposed to predominantly bulk species ($C_n \leq 6$).

While fatty acids have implications in many fields such as biological membranes,^{17–19} mineral flotation,^{20,21} and food science,^{22–24} of particular interest is aerosol chemistry. Breaking waves at the ocean surface generate and release sea spray aerosols (SSA) to the neighboring atmosphere. During this process, the organic molecules enriched in the sea surface microlayer (SSML) are transferred to the atmosphere as coatings on SSA. Although C_{16} and C_{18} fatty acids are found to be the most abundant in these organic films,^{13,25,26} C_8 – C_{10} saturated fatty acids have also been identified in significant concentrations.¹³ Moreover, the concentrations of these shorter acids are likely to become more prevalent as the aerosol ages due to the oxidation of longer-chain fatty acids.^{27–30}

SSA reactivity,^{31–34} lifetime,^{35,36} light-scattering^{37,38} and nucleating abilities³⁹ are affected by the organic coatings at the aerosol–atmosphere interface. Surface tension is one of the governing parameters of several of these properties, and can be affected by the pH of the aerosol, and in turn, the surface- pK_a of the molecules at the interface. Upon entering the atmosphere, SSA will be at a pH close to that of the ocean (8.1),⁴⁰ and any short- or medium-chain fatty acids have been thought to exist in their deprotonated state, and therefore would have low surface activity. However, upon aging in the atmosphere, reactions with gas phase acidic species (*i.e.* HCl, HNO₃) will cause these aerosols to become acidified,⁴¹ thus increasing the surface activity of the fatty acids and decreasing the surface tension at the interface. The pH at which this transformation (deprotonated to protonated) occurs is dictated by the surface- pK_a of the species at the interface, and will affect the surface tension-dependent properties of the aerosol. For example, separation relative humidity (SRH) is a metric that can be used to determine the phase state of an aerosol, and is affected by pH and the pK_a of the organic fraction of SSA. The SRH of model SSA particles decreases at high pH as a result of the increased solubility of the organic components.⁴² As particle phase state has a large influence on the chemical and physical properties of an aerosol, an understanding of the pH at which the organic components become deprotonated is crucial.⁴³

The primary goal of this work is to determine the surface- pK_a of medium-chain fatty acids at the air–water interface, which we expect to differ from their commonly used bulk values (~ 4.8). We utilize a surface tension titration technique to determine these values, and evaluate our results within the context of similar, yet controversial, studies in the literature.

Experimental methods

Materials

Octanoic acid (C_8 , $\geq 99\%$, M_w 144.21 g mol⁻¹), nonanoic acid (C_9 , $\geq 97\%$, M_w 158.24 g mol⁻¹), and decanoic acid (C_{10} , $\geq 98\%$,

M_w 172.26 g mol⁻¹) were purchased from Sigma Aldrich (St. Louis, MO) and used without further purification. HCl (Trace Metal Grade) was purchased from Fisher Scientific (Waltham, MA), and NaOH pellets (99%) were purchased from Mallinckrodt (Paris, KY). A Barnstead Nanopure filtration system (D4741, Thermolyne Corporation, Dubuque, IA) with additional cartridges to remove organic material (D5026 Type I ORGANIC-free Cartridge Kit, Pretreat Feed) provided ultrapure water with a resistivity of at least 18.0 M Ω cm. Solutions of the C_8 – C_{10} acids were prepared at concentrations of 1 mM at pH 12 for surface tension (γ) *versus* pH titrations with a 0.10 M HCl titrant. The C_9 system was also prepared at 1 mM in a pH 2 solution for titration with 0.10 M NaOH. 1 mM C_9 solutions were prepared in ultrapure water for standard acid–base titrations with 0.005 M NaOH. All experiments were conducted at 21 ± 1 °C and at a measured relative humidity of $43 \pm 2\%$.

Surface tension measurements

Surface tension was probed with a platinum Wilhelmy plate and calculated *via*

$$\gamma = \frac{F}{l \times \cos \theta} \quad (1)$$

where the force (F) is obtained from the measured difference in mass of the plate, θ is the contact angle between the plate and solution (assumed to be 0°),⁴⁴ and l is the perimeter of the wetted surface (39.24 mm). Readings were obtained with a KSV NIMA (Biolin Scientific, Espoo, Finland) tensiometer and interface unit equipped with LayerBuilder software. The plate was heated by flame prior to measurements to remove any organic residue from the surface.

Surface tension titration

The use of surface tension to determine surface- pK_a was inspired by the work Dickhaus & Priefer and Sugawara *et al.*^{45,46} For the C_8 – C_{10} acids, surface tension *versus* pH data was obtained *via* titration of a 50 mL aliquot of the C_n solution with either acid or base while monitoring γ and pH (Accumet AB15 pH meter, Fisher Scientific). The pH probe was calibrated before the measurements with pH 1, 4, 6, 7, and 10 buffer solutions. The γ measurements were taken continuously as titrant was added to a 1 mM aliquot of fatty acid solution, allowing for the mass reading to stabilize before a measurement was recorded. Stirring was used to ensure efficient mixing of the added titrant. For titrant additions after which the mass reading did not change significantly, a wait time of 2 minutes was allotted prior to recording the surface tension mass reading. Along more dynamic areas of the titration curves, an equilibration time of at least 10 minutes was required for the mass readings to stabilize. A reading was deemed stable when the mass only changed by approximately 2 mg around a central value. Dilution effects⁴⁷ on the measured γ of the Gibbs monolayer were minimized with only a $\sim 10\%$ increase in volume from titrant addition (Fig. S1 and S2, ESI[†]). To compensate for the rising height of solution due to the addition of titrant, the plate was periodically raised to maintain a constant depth in solution. The error bars reported are dominated by the uncertainties from

the pH meter measurements and the error of the surface tension data fits. Errors reported represent one standard deviation from the average of triplicate measurements.

Infrared reflection absorption spectroscopy

To probe the structure and ordering of the surfactant films at the interface, IRRAS spectra of the C_9 systems were collected using a custom built setup housed in an FTIR spectrometer (Spectrum 100, Perkin Elmer). The setup consists of two gold mirrors. The first mirror directs the incoming IR beam to the sample surface at an incidence angle of 46° relative to surface normal. The second mirror directs the reflected beam to a liquid nitrogen-cooled MCT detector. As IRRAS spectra are plotted in terms of reflectance-absorbance ($RA = -\log(R/R_0)$), a background spectrum was collected of a bare pH 2, 5.6 (water), or 12 surface and used as R_0 . This background solution was aspirated from the Petri dish and replaced with a 1 mM C_9 solution at the appropriate pH. The spectrum of this solution was used as R . Spectra of the C_9 systems were compared to that of a stearic acid (C_{18}) monolayer. Each spectrum is the result of coaveraging 300 scans over the full range ($4000\text{--}450\text{ cm}^{-1}$) at a resolution of 4 cm^{-1} . Spectra shown have been baseline-subtracted by a third order polynomial and are the average of at least 3 individual spectra.

Results & discussion

C_n titration with 0.10 M HCl

To experimentally determine the surface- pK_a of the $C_8\text{--}C_{10}$ medium-chain fatty acids, 1 mM solutions were titrated with 0.10 M HCl from a pH of 12 to a pH of 2. Representative surface tension vs. pH titration curves for the three acids are shown in Fig. 2. At a pH of 12, the C_n acids are fully deprotonated, and thus relatively surface inactive. The surface tension curves begin at pH 12 and at surface tensions of approximately 70 mN m^{-1} , slightly depressed relative to pure water. As 0.10 M HCl is titrated into the solutions, the surface tension decreases, indicative of the formation of the more surface-active protonated species. The C_8 and C_9 curves develop an interesting feature from pH 6 to 4.5, hereafter referred to as the surface tension dip, where the surface tension decreases to a minimum value then rises to reach a plateau. The physical interpretation of this dip is discussed later.

Upon titration to $\text{pH} < 4$, the surface tension curves approach constant values. The values of surface tension at this point reflect the relative surface activity of each C_n acid. C_{10} approaches a surface tension value of $33.1 \pm 0.3\text{ mN m}^{-1}$ (the most surface active), followed by C_9 at $34.3 \pm 1.6\text{ mN m}^{-1}$, and C_8 at $52.9 \pm 2.7\text{ mN m}^{-1}$. The greater surface activity with chain length can be attributed to increasing van der Waals forces between the longer hydrocarbon chains.

A mathematical model is applied to the collected surface tension titration data to calculate the surface- pK_a ($pK_{a(s)}$) of the selected C_n fatty acids. This model (described in Appendix A) is adapted from that of Cratin⁴⁸ in his work on the interfacial pK_a

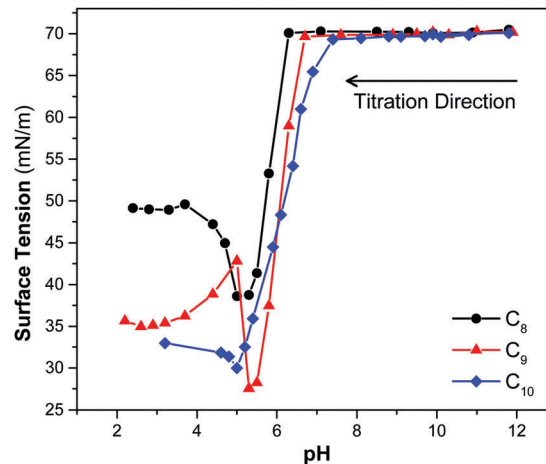


Fig. 2 Surface tension vs. pH titration curves for 1 mM C_8 (black circles), C_9 (red triangles), and C_{10} (blue diamonds) fatty acid solutions. The titration is conducted from high pH to low pH via the addition of 0.10 M HCl to the 1 mM C_n solutions originally at pH 12. Lines between data points are drawn to guide the eye.

of stearic acid at the oil-water interface, and is expressed in terms of the change in surface tension with pH.

$$\Delta\gamma = \frac{\Delta\gamma_{\max}}{1 + 10^{(\text{pH}_b - \text{p}K_{a(s)})}} \quad (2)$$

When this surface activity model is applied to the systems studied here, a trend is observed between the surface- pK_a and chain length. The fits of the data are shown in Fig. 3 and the surface- pK_a values of the C_n systems are presented in Table 1. As can be seen from the values in Table 1, the surface- pK_a of the fatty acid increases with chain length from 4.9 to 6.4. This trend can be understood to be an additional consequence of increased van der Waals forces between fatty acid molecules with longer chains. Greater forces between the hydrophobic groups at the interface result in increased interactions between the carboxylate headgroups, thus making the acidic hydrogen more difficult to remove.³ However, the surface- pK_a for the C_8 system (4.9 ± 0.2) is within the range of the accepted value of its bulk pK_a (4.89).¹⁴ When a 1 mM C_9 system, prepared in water, is titrated with NaOH in a standard weak acid-strong base titration (Fig. S3, ESI[†]), a bulk pK_a of 4.97 ± 0.05 is determined from the pH at the half-way point, which also is in close agreement with its literature pK_a value of 4.96.¹⁴ The significant deviation of surface- pK_a from the C_9 bulk value demonstrates that our surface tension titration is actually probing the surface- pK_a at the air-aqueous interface. The surface- pK_a values presented here should be used when discussing surface speciation.

Although the trend observed with chain length is in accordance with accepted trends in the literature,^{3,11} the surface- pK_a values obtained via our surface tension titration are lower than those which have been reported for the C_8 and C_{10} acids by Kanicky *et al.*³ Throughout the literature, there are many values reported for the pK_a of both medium- and long-chain fatty acids, although less have been reported for the former. A summary of these results, in addition to those determined here, are represented in Fig. 4.

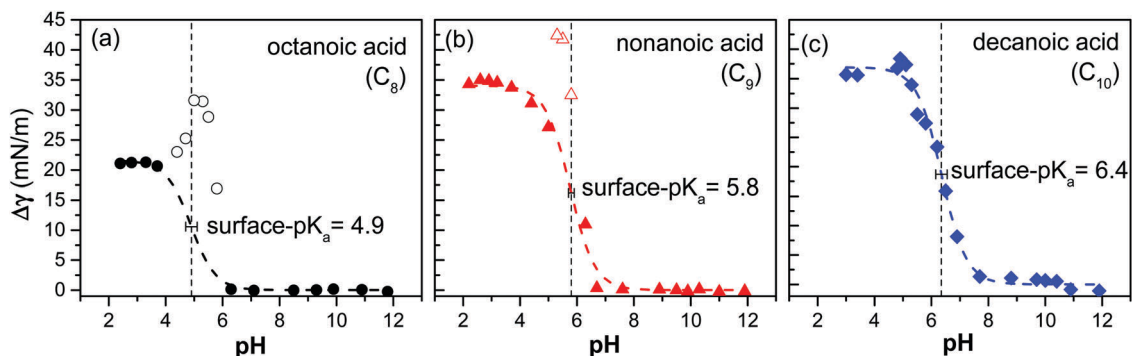


Fig. 3 The surface activity model (dashed line along data points) applied to C_8 (a), C_9 (b), and C_{10} (c) systems. The vertical dashed line is the average surface- pK_a and includes an error bar of \pm one standard deviation based on the calculation of surface- pK_a for three separate trials. Surface tension data has been transformed to $\Delta\gamma = \gamma_{\max} - \gamma$.

Table 1 Surface- pK_a of C_8 – C_{10} fatty acids titrated from pH 12 with 0.10 M HCl

C_n	Surface- pK_a ($pK_{a(s)}$)
C_8	4.9 ± 0.2
C_9	5.8 ± 0.1
C_{10}	6.4 ± 0.2

These values have been determined using a variety of techniques, cover a wide range, and are only sometimes specifically designated as the surface- pK_a . Acid–base titration techniques, not including surface tension, were utilized by Kanicky,³ McLean,¹¹ and Cistola⁸ to determine the pK_a of fatty acids with chain lengths up to eighteen carbons. McLean studied high concentrations of fatty acids to determine “colloidal pK_a ,” and obtained values that are significantly lower than those obtained by Kanicky, particularly at shorter carbon chain lengths. However, a linear trend of increasing pK_a with chain length is consistent between the works.

Other techniques for determining the protonation state of surface-active fatty acids can also be applied to calculate surface- pK_a . For example, using X-ray photoelectron spectroscopy, Prisle *et al.*⁴⁹

found the fraction of 0.03 M decanoic acid in a decanoic acid/decanoate system to be only $\sim 10\%$ at a bulk pH of 7.1. When the Henderson–Hasselbalch equation is applied to the published data, a surface- pK_a value of 6.1 is calculated for their C_{10} system, which agrees well with the value reported here. Monolayer relaxation data and surface potential-area isotherms were used by Aveyard *et al.* and Glazer *et al.* to calculate the surface- pK_a of stearic acid as 9.5 and 8.0, respectively.^{50,51} Overall, these results suggest inconsistencies in the determination of surface- pK_a between measurement techniques.

The work of Kanicky, McLean, and Prisle also imply that concentration can impact the determination of surface- pK_a , as concentrations of the systems vary amongst the experiments and sometimes are not specified in the literature. Additionally, in those experiments in which acid–base titration is used to determine pK_a , concentration variations between the studies may affect the activity coefficient of the ionized species in such a way that could potentially account for discrepancies in the reported pK_a values.^{9,52} It has been shown that upon dilution of medium-chain fatty acid systems, and subsequent extrapolation of the data to an extremely dilute limit, the pK_a of these acids approach a value of approximately 5.0.⁵³ The 1 mM concentrations used in the experiments presented here lie at the solubility limit for the C_8 – C_{10} acids in water.¹⁵ Therefore, the values reported in Table 1 represent the upper limit to the surface- pK_a of these systems.

In Fig. 3, it can be seen that the surface- pK_a of the C_8 and C_9 systems are near the pH values where the surface tension dips are observed during the titrations. Similar surface tension dip features with oleic acid/sodium oleate systems have been observed elsewhere in the literature, and are important in the field of mineral flotation.^{54–56} Surface tension minima were observed at pH values of approximately 9–10 in the various reports, corresponding to the surface- pK_a of oleic acid.⁵⁷ This minimum in surface tension is caused by maximum interactions between the acid ($RCOOH$) and dissociated soap ($RCOO^-$) species, resulting in acid–soap complexes ($RCOOH:RCOO^-$) at the interface, which are more surface active than simply the acid species.^{53,56,58} The surface tension dip results obtained here for the C_8 and C_9 systems agree with these reports in that the surface tension minima are observed near pH values associated with, but not at,

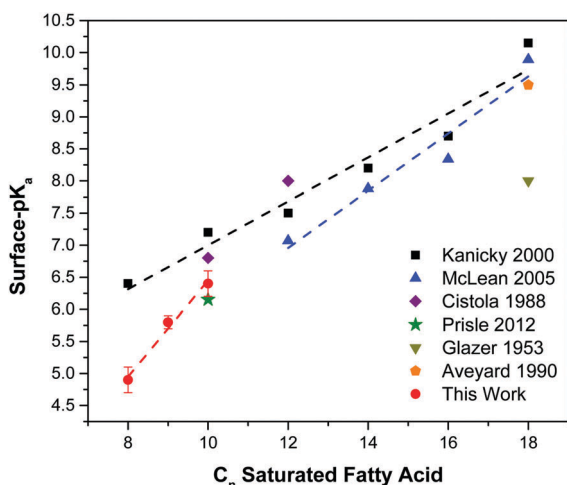


Fig. 4 Survey of surface- pK_a values from the literature.^{3,8,11,49–51} Dashed lines are linear fits of selected data sets and are drawn to guide the eye.

the respective surface- pK_a of the acid systems. From knowledge of the oleic acid systems, we also assume that the cause of the minima in the C_8 and C_9 systems is the presence of $\text{RCOOH}:\text{RCOO}^-$ complexes at the interface. Interestingly, a dip was not observed for the C_{10} system. It is plausible that acid–soap complexes exist, but are not necessarily more surface active than the acid alone in the C_{10} system. It is important to note that the data points along the titration curve that are associated with the surface tension dip for the C_8 and C_9 systems were removed prior to fitting the data with eqn (2). This is due to an assumption within the surface activity model that all species, protonated or deprotonated, exist ideally in solution or at the interface with only weak interactions.⁴⁸ As it is assumed that this dip is due to the strong interaction of acid–soap species, the deviation from the fit of the data with eqn (2) is further evidence of the formation of $\text{RCOOH}:\text{RCOO}^-$ complexes near the surface- pK_a .

C_9 titration with 0.10 M NaOH

The titration curves obtained in this work are not the result of measuring several solutions made at discrete pH values. Therefore, the impact of the direction of the titration was considered by titrating a 1 mM C_9 solution at pH 2 with 0.10 M NaOH to approach pH 12. A representative titration of this kind is depicted in Fig. 5. The fully protonated C_9 solution has a surface tension of $31.4 \pm 2.0 \text{ mN m}^{-1}$ prior to the titration. The similarity between this starting value and the final value around pH 2 of C_9 in Fig. 2 supports the claim that dilution of the C_n solutions over the course of the HCl titration has a minimal impact on the overall results. As the solution becomes more basic during the titration, the surface tension rises as the C_9 species become deprotonated and are removed from the interface. At high pH values, the surface tension approaches a value of approximately 69 mN m^{-1} , in agreement with the starting point of the titration of C_9 with 0.10 M HCl.

Noticeably absent from Fig. 5a is the surface tension dip observed in the C_9 titration curve in Fig. 2. As stated previously, this dip in surface tension is due to the formation of $\text{RCOOH}:\text{RCOO}^-$ complexes near the surface- pK_a . However, as a pH 2 solution of C_9 is titrated with 0.10 M NaOH, the concentration of Na^+ ions in the resulting solution is much greater than the concentration of Na^+ that is diluted in the titration of a pH 12 solution with 0.10 M HCl. For example, the concentration of Na^+ at pH ~ 5 is roughly double in the titration with 0.10 M NaOH compared to that with 0.10 M HCl, respectively $18.5 \pm 0.3 \text{ mM}$ and $9.1 \pm 0.1 \text{ mM}$. The increase in Na^+ concentration leads to a disruption in the hydrogen bonding network between protonated and deprotonated fatty acids, similar to a recent study of the effect of sodium on palmitic acid monolayers at varying degrees of deprotonation.⁵⁹ This change in bonding environment prevents the complexation, thus eliminating the observed dip.

When eqn (2) is applied to the C_9 titration with 0.10 M NaOH (Fig. 5b), a surface- pK_a value of 5.21 ± 0.02 is determined. When compared to the surface- pK_a obtained using the acidic titrant, the results have a ΔpK_a of -0.6 . The likely cause for such a change in the surface- pK_a is the higher concentration of

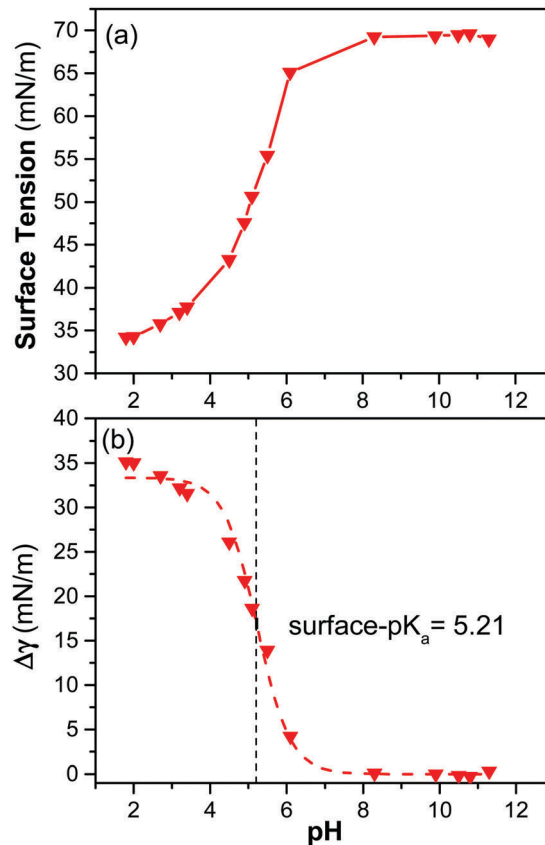


Fig. 5 Surface tension vs. pH titration curve of 1 mM C_9 solution at pH 2 with 0.10 M NaOH. The solid line in (a) is to guide the eye. The dashed line through the data points in (b) is the curve generated by fitting the data to eqn (2). The vertical dashed line is the calculated average surface- pK_a .

Na^+ in solution. While the Gouy–Chapman model^{60–62} was not used to calculate the surface- pK_a of these weakly packed (Fig. 6 and Fig. S5, ESI†) Gibbs monolayer systems,⁶³ the Poisson–Boltzmann description of ion distribution at the interface sheds light on the reduced surface- pK_a in the presence of additional Na^+ . According to Gouy–Chapman theory, at a given pH, the addition of competing monovalent ions to a system will result in a decreased amount of H^+ ions accumulating at the interface. Therefore, there will be an increased tendency for the acidic groups at the interface to deprotonate.⁶² As there is a greater concentration of Na^+ in this direction of titration at pH values near the surface- pK_a , the shift of the surface- pK_a to a lower value is to be expected. This effect of ions on surface- pK_a has been observed elsewhere in the literature. In the work of Aveyard *et al.*, the surface- pK_a of stearic acid was found to decrease by 2 pH units upon the addition of 10 mM NaCl ⁵⁰ (roughly the same amount as the difference between the acidic and basic titrant systems here). By tracking changes in the vibrational modes associated with the hydrogen-bonded carbonyl ($\text{C}=\text{O}$) and the deprotonated carboxylate (CO_2^-) headgroup of acid and deprotonated forms, respectively, spectroscopic investigations, utilizing IRRAS and vibrational sum frequency generation (VSFG), have also revealed that ions (Na^+ , Ca^{2+} , Mg^{2+} , Zn^{2+} , *etc.*) can affect the protonation state of fatty acid monolayers at

the air–aqueous interface.^{61,64–66} This is, again, due to a reduction in the surface- pK_a as a result of ion affinity for the negative electron density of the carboxylate headgroups at the surface. Therefore, it is important to acknowledge that the concentration of ions in solution will have an effect on the surface- pK_a determined *via* surface tension titration and other methods.

Conclusions

We have used surface tension titration to determine the surface- pK_a of C_8 – C_{10} medium-chain fatty acids at the air–water interface. The surface tension *versus* pH data was fit to a surface activity model⁴⁸ which determined surface- pK_a values of 4.9 for octanoic acid, 5.8 for nonanoic acid, and 6.4 for decanoic acid. Due to the solubility limit of the acids in water, these values represent the upper limit to the surface- pK_a , which decreases upon dilution of the system to the value of the bulk pK_a . The octanoic and nonanoic acid systems exhibited a surface tension dip near the surface- pK_a due to the formation of acid–soap complexes, which have greater surface activity than the pure acid form. Additionally, it was shown that even small amounts of Na^+ can lower the surface- pK_a of the C_9 acid system (5.2), and disrupt the bonding network between acid and soap species. This general result is consistent with the ion-induced deprotonation of various fatty acid systems due to the distribution of ions at a charged interface.^{61,64–66} Upon comparison of the results presented here with those currently in the literature,^{3,8,11,49} there still exists controversy.

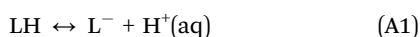
The surface- pK_a of fatty acids deviates significantly from the bulk value of acetic acid starting at a chain length of nine carbon atoms. Moreover, the surface- pK_a of these fatty acids are not equivalent to their values in the bulk, as evidenced by the weak acid–strong base titration of nonanoic acid which resulted in a bulk pK_a value of 4.97, consistent with what has been reported in the literature.¹⁴ Therefore, the values of the surface- pK_a of the SSA-prevalent soluble fatty acids determined here should be utilized for aerosol reactivity and CCN models to more accurately assign the speciation, and surface activity, of organic components at the surface of SSA.^{39,67,68} Such advances in the understanding of the fundamental properties of these interfacial systems will help to improve certainty in the impacts of aerosols on the climate.

Conflicts of interest

The authors declare no conflict of interest for this manuscript.

Appendix A. Surface activity model derivation

If one considers the equilibrium between the protonated (LH) and deprotonated (L^-) forms of a C_n acid at the surface,



the following expression for the surface equilibrium constant, $K_{a(s)}$, is obtained.

$$K_{a(s)} = \frac{[L^-]_s [H^+]_s}{[LH]_s} \quad (A2)$$

From the equilibrium, the fraction of protonated (f_{LH}) and deprotonated (f_{L^-}) species can be written as

$$f_{LH} = \frac{[LH]_s}{[L^-]_s + [LH]_s} \quad (A3a)$$

$$f_{L^-} = \frac{[L^-]_s}{[L^-]_s + [LH]_s} \quad (A3b)$$

and rearranged to be expressed in terms of $K_{a(s)}$ and $[H^+]_s$.

$$f_{LH} = \frac{1}{1 + K_{a(s)}[H^+]_s^{-1}} \quad (A4a)$$

$$f_{L^-} = \frac{K_{a(s)}[H^+]_s^{-1}}{1 + K_{a(s)}[H^+]_s^{-1}} \quad (A4b)$$

Or, using the definitions of pH and pK_a , eqn (A4a) and (A4b) can be rewritten as

$$f_{LH} = \frac{1}{1 + 10^{(pH_s - pK_{a(s)})}} \quad (A5a)$$

$$f_{L^-} = \frac{10^{(pH_s - pK_{a(s)})}}{1 + 10^{(pH_s - pK_{a(s)})}} \quad (A5b)$$

It is important to note that in order to apply Cratin's surface activity model⁴⁸ (originally developed to describe stearic acid dissociation at the oil–water interface where a completely dissociated acid would result in an interfacial tension of $\sim 0 \text{ mN m}^{-1}$) to these systems, a simple difference must be taken within the data such that at high pH, the surface tension is associated with a value of 0 mN m^{-1} . As such, the surface tension data collected during the titration is presented as $\Delta\gamma$ against pH, where $\Delta\gamma = \gamma_{\max} - \gamma$, and γ_{\max} is the surface tension of the C_n system at a pH of 12. The surface activity (a) for these medium-chain fatty acids at the air–water interface is then expressed in terms of the lowering of this surface tension difference relative to a maximum value ($\Delta\gamma_{\max}$, obtained at low pH).

$$a = \frac{(\Delta\gamma_{\max} - \Delta\gamma)}{\Delta\gamma_{\max}} \quad (A6)$$

One of the bounds of this model is that all species, protonated or deprotonated, must coexist independently with only weak interactions in order to express their total activity as a simple summation. Under this assumption, the total activity (a_t) of the system can be expressed as the sum of the activity and fraction of the protonated and deprotonated species.

$$a_t = \sum_i a_i f_i = a_{L^-} f_{L^-} + a_{LH} f_{LH} \quad (A7)$$

Equating eqn (A6) and (A7) yields

$$\frac{(\Delta\gamma_{\max} - \Delta\gamma)}{\Delta\gamma_{\max}} = a_{L^-}f_{L^-} + a_{LH}f_{LH} \quad (\text{A8})$$

From examination of a $\Delta\gamma$ vs. pH plot for these systems, one can deduce that $a_{LH} = 0$, and $a_{L^-} = 1$ (see ESI[†]). From this, eqn (A8) can be written as

$$\frac{(\Delta\gamma_{\max} - \Delta\gamma)}{\Delta\gamma_{\max}} = f_{L^-} \quad (\text{A9})$$

which can be arranged and expressed as eqn (A10).

$$\Delta\gamma = \Delta\gamma_{\max}(1 - f_{L^-}) \quad (\text{A10})$$

Inserting the equation for f_{L^-} from eqn (A5b), the above equation can be written in terms of the surface pH (pH_s) and $\text{p}K_{a(s)}$ of the system.

$$\Delta\gamma = \Delta\gamma_{\max} \left(1 - \frac{10^{(\text{pH}_s - \text{p}K_{a(s)})}}{1 + 10^{(\text{pH}_s - \text{p}K_{a(s)})}} \right) \quad (\text{A11})$$

Finally, eqn (A11) can be simplified to yield

$$\Delta\gamma = \frac{\Delta\gamma_{\max}}{1 + 10^{(\text{pH}_s - \text{p}K_{a(s)})}} \quad (\text{A12})$$

If one assumes that pH_s is equal to the bulk pH (pH_b), eqn (A12) becomes

$$\Delta\gamma = \frac{\Delta\gamma_{\max}}{1 + 10^{(\text{pH}_b - \text{p}K_{a(s)})}}$$

While charged monolayers at the interface can create an electric double layer with hydrogen ion concentrations enhanced relative to the bulk, a 1 mM C_9 solution, for example, represents a very loosely packed sub-monolayer system. Fig. 6 shows IRRAS spectra of 1 mM C_9 solutions at pH 2, 12, and of samples extracted from the titration experiment at the surface tension dip. No CH stretching modes are observed at pH 12 indicating that the C_9 molecules are not found above the

detection limit at the interface. CH stretching modes are present for the 1 mM C_9 solution at pH 2 and in the extracted dip region sample. However, the intensities of the modes are very weak, and the CH_2 stretching frequencies are blue shifted compared to more ordered and surface active monolayer of stearic acid (Fig. S5, ESI[†]), indicating that the C_9 system is loosely packed and exhibits significant gauche defects. Therefore, the assumption that pH_s is approximately equal to pH_b holds for the calculation of the surface- $\text{p}K_a$ of the medium-chain fatty acids.⁶³

Acknowledgements

This research was supported under Grant CHE-1305427 from the National Science Foundation via the Center for Aerosol Impacts on Chemistry of the Environment. The authors are grateful to Dr. Dominique Verreault for guidance and discussion of various surface- $\text{p}K_a$ calculations. The authors would also like to thank Dr. Ellen Adams for helpful discussions regarding this work.

References

- 1 K. B. Eisenthal, *Chem. Rev.*, 1996, **96**, 1343–1360.
- 2 H.-J. Butt, K. Graf and M. Kappl, *Physics and Chemistry of Interfaces*, Wiley-VCH, Weinheim, 2013.
- 3 J. R. Kanicky, A. F. Poniatowski, N. R. Mehta and D. O. Shah, *Langmuir*, 2000, **16**, 172–177.
- 4 E. C. Griffith and V. Vaida, *J. Am. Chem. Soc.*, 2013, **135**, 710–716.
- 5 H. F. Wang, X. L. Zhao and K. B. Eisenthal, *J. Phys. Chem. B*, 2000, **104**, 8855–8861.
- 6 X. L. Zhao, S. W. Ong, H. F. Wang and K. B. Eisenthal, *Chem. Phys. Lett.*, 1993, **214**, 203–207.
- 7 M. P. Andersson, M. H. M. Olsson and S. L. S. Stipp, *Langmuir*, 2014, **30**, 6437–6445.
- 8 D. P. Cistola, J. A. Hamilton, D. Jackson and D. M. Small, *Biochemistry*, 1988, **27**, 1881–1888.
- 9 C. J. Drummond, F. Grieser and T. W. Healy, *J. Chem. Soc., Faraday Trans. 1*, 1989, **85**, 521–535.
- 10 C. R. Whiddon, C. A. Bunton and O. Soderman, *J. Phys. Chem. B*, 2003, **107**, 1001–1005.
- 11 D. S. McLean, D. Vercoe, K. R. Stack and D. Richardson, *Appita J.*, 2005, **58**, 362–366.
- 12 R. Ciuraru, L. Fine, M. van Pinxteren, B. D'Anna, H. Herrmann and C. George, *Sci. Rep.*, 2015, **5**, 12741.
- 13 R. E. Cochran, O. Laskina, T. Jayarathne, A. Laskin, J. Laskin, P. Lin, C. Sultana, C. Lee, K. A. Moore, C. D. Cappa, T. H. Bertram, K. A. Prather, V. H. Grassian and E. A. Stone, *Environ. Sci. Technol.*, 2016, **50**, 2477–2486.
- 14 W. M. Haynes and D. R. Lide, *CRC handbook of chemistry and physics: a ready-reference book of chemical and physical data*. CRC Press, Boca Raton, 2011.
- 15 A. W. Ralston and C. W. Hoerr, *J. Org. Chem.*, 1942, **7**, 546–555.

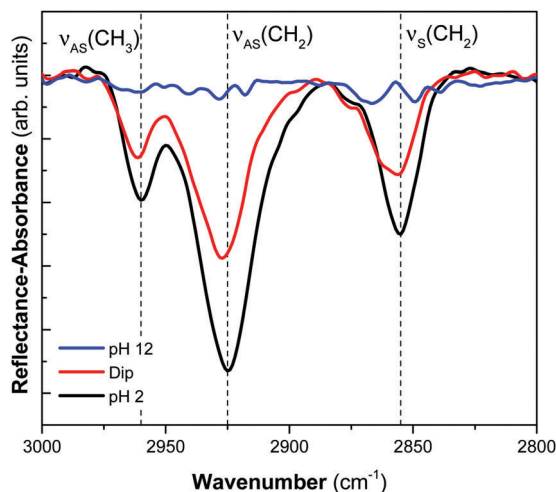


Fig. 6 IRRAS spectra in the CH stretching region of 1 mM solutions of C_9 at pH 12 (blue, top), solution extracted from the surface tension dip of a titration with 0.10 M HCl (red), and at pH 2 (black).

- 16 P. Mukerjee and K. J. Mysels, *Critical Micelle Concentrations in Aqueous Surfactant Systems*, National Bureau of Standards, NSRDS-NBS 36, Washington, D. C., 1971.
- 17 F. Kamp, H. V. Westerhoff and J. A. Hamilton, *Biochemistry*, 1993, **32**, 11074–11086.
- 18 R. Schmidt, U. Meier, M. Yabut-Perez, D. Walmrath, F. Grimminger, W. Seeger and A. Gunther, *Am. J. Respir. Crit. Care Med.*, 2001, **163**, 95–100.
- 19 E. Sparr, L. Eriksson, J. A. Bouwstra and K. Ekelund, *Langmuir*, 2001, **17**, 164–172.
- 20 R. C. Guimaraes, A. C. Araujo and A. E. C. Peres, *Miner. Eng.*, 2005, **18**, 199–204.
- 21 K. H. Rao and K. S. E. Forssberg, *Miner. Eng.*, 1991, **4**, 879–890.
- 22 D. J. McClements and E. A. Decker, *J. Food Sci.*, 2000, **65**, 1270–1282.
- 23 H. T. Osborn and C. C. Akoh, *Food Chem.*, 2004, **84**, 451–456.
- 24 T. Waraho, D. J. McClements and E. A. Decker, *Food Chem.*, 2011, **129**, 854–859.
- 25 M. Mochida, Y. Kitamori, K. Kawamura, Y. Nojiri and K. Suzuki, *J. Geophys. Res.: Atmos.*, 2002, **107**, 4325.
- 26 H. Tervahattu, K. Hartonen, V. M. Kerminen, K. Kupiainen, P. Aarnio, T. Koskentalo, A. F. Tuck and V. Vaida, *J. Geophys. Res.: Atmos.*, 2002, **107**, 4053.
- 27 E. Gonzalez-Labrada, R. Schmidt and C. E. DeWolf, *Phys. Chem. Chem. Phys.*, 2007, **9**, 5814–5821.
- 28 M. D. King, A. R. Rennie, K. C. Thompson, F. N. Fisher, C. C. Dong, R. K. Thomas, C. Pfrang and A. V. Hughes, *Phys. Chem. Chem. Phys.*, 2009, **11**, 7699–7707.
- 29 A. K. Y. Lee and C. K. Chan, *Atmos. Environ.*, 2007, **41**, 4611–4621.
- 30 L. F. Voss, M. F. Bazerbashi, C. P. Beekman, C. M. Hadad and H. C. Allen, *J. Geophys. Res.: Atmos.*, 2007, **112**, D06209.
- 31 A. Rouviere and M. Ammann, *Atmos. Chem. Phys.*, 2010, **10**, 11489–11500.
- 32 O. S. Ryder, N. R. Campbell, M. Shalowski, H. Al-Mashat, G. M. Nathanson and T. H. Bertram, *J. Phys. Chem. A*, 2015, **119**, 8519–8526.
- 33 M. A. Shalowski, T. B. Sobyra and G. M. Nathanson, *J. Phys. Chem. A*, 2015, **119**, 12357–12366.
- 34 K. Stemmler, A. Vlasenko, C. Guimbaud and M. Ammann, *Atmos. Chem. Phys.*, 2008, **8**, 5127–5141.
- 35 J. F. Davies, R. E. H. Miles, A. E. Haddrell and J. P. Reid, *Proc. Natl. Acad. Sci. U. S. A.*, 2013, **110**, 8807–8812.
- 36 W. D. Garrett, *J. Atmos. Sci.*, 1971, **28**, 816–819.
- 37 C. Pilinis, S. N. Pandis and J. H. Seinfeld, *J. Geophys. Res.: Atmos.*, 1995, **100**, 18739–18754.
- 38 C. A. Randles, L. M. Russell and V. Ramaswamy, *Geophys. Res. Lett.*, 2004, **31**, L16108.
- 39 C. R. Ruehl, J. F. Davies and K. R. Wilson, *Science*, 2016, **351**, 1447–1450.
- 40 F. J. Millero, *Chemical Oceanography*, CRC Press, Boca Raton, 3rd edn, 2006.
- 41 W. C. Keene, A. A. P. Pszenny, J. R. Maben, E. Stevenson and A. Wall, *J. Geophys. Res.: Atmos.*, 2004, **109**, D23307.
- 42 D. J. Losey, R. G. Parker and M. A. Freedman, *J. Phys. Chem. Lett.*, 2016, **7**, 3861–3865.
- 43 M. Bilde and B. Svenningsson, *Tellus, Ser. B*, 2004, **56**, 128–134.
- 44 K. Holmberg, D. O. Shah and M. J. Schwuger, *Handbook of Applied Surface and Colloid Chemistry*, Wiley, New York, 2002.
- 45 B. N. Dickhaus and R. Priefer, *Colloids Surf., A*, 2016, **488**, 15–19.
- 46 M. Sugawara, K. Isazawa and T. Kambara, *Fresenius' J. Anal. Chem.*, 1981, **308**, 17–20.
- 47 K. D. Danov, P. A. Kralchevsky, K. P. Ananthapadmanabhan and A. Lips, *J. Colloid Interface Sci.*, 2006, **300**, 809–813.
- 48 P. D. Cratin, *J. Dispersion Sci. Technol.*, 1993, **14**, 559–602.
- 49 N. L. Prisle, N. Ottosson, G. Öhrwall, J. Söderström, M. Dal Maso and O. Björneholm, *Atmos. Chem. Phys.*, 2012, **12**, 12227–12242.
- 50 R. Aveyard, B. P. Binks, N. Carr and A. W. Cross, *Thin Solid Films*, 1990, **188**, 361–373.
- 51 J. Glazer and M. Z. Dogan, *Trans. Faraday Soc.*, 1953, **49**, 448–455.
- 52 D. C. Harris, *Quantitative Chemical Analysis*, W. H. Freeman and Company, New York, 3rd edn, 1991.
- 53 J. R. Kanicky and D. O. Shah, *Langmuir*, 2003, **19**, 2034–2038.
- 54 A. Atrafi and M. Pawlik, *Miner. Eng.*, 2016, **85**, 138–147.
- 55 F. H. B. DeCastro and A. G. Borrego, *J. Colloid Interface Sci.*, 1995, **173**, 8–15.
- 56 R. Pugh and P. Stenius, *Int. J. Miner. Process.*, 1985, **15**, 193–218.
- 57 J. R. Kanicky and D. O. Shah, *J. Colloid Interface Sci.*, 2002, **256**, 201–207.
- 58 J. Rudin and D. T. Wasan, *Colloids Surf.*, 1992, **68**, 81–94.
- 59 E. M. Adams, B. A. Wellen, R. Thiriaux, S. K. Reddy, A. S. Vidalis, F. Paesani and H. C. Allen, *Phys. Chem. Chem. Phys.*, 2017, **19**, 10481–10490.
- 60 J. N. Israelachvili, *Intermolecular and Surface Forces*, Academic Press, New York, 2011.
- 61 E. Le Calvez, D. Blaudez, T. Buffeteau and B. Desbat, *Langmuir*, 2001, **17**, 670–674.
- 62 K. Spildo and H. Høiland, *J. Colloid Interface Sci.*, 1999, **209**, 99–108.
- 63 M. Egret-Charlier, A. Sanson, M. Ptak and O. Bouloussa, *FEBS Lett.*, 1978, **89**, 313–316.
- 64 E. J. Robertson, D. K. Beaman and G. L. Richmond, *Langmuir*, 2013, **29**, 15511–15520.
- 65 J. Simon-Kutscher, A. Gericke and H. Hühnerfuss, *Langmuir*, 1996, **12**, 1027–1034.
- 66 C. Y. Tang, Z. Huang and H. C. Allen, *J. Phys. Chem. B*, 2010, **114**, 17068–17076.
- 67 S. M. Burrows, O. Ogunro, A. A. Frossard, L. M. Russell, P. J. Rasch and S. M. Elliott, *Atmos. Chem. Phys.*, 2014, **14**, 13601–13629.
- 68 S. M. Burrows, E. Gobrogge, L. Fu, K. Link, S. M. Elliott, H. F. Wang and R. Walker, *Geophys. Res. Lett.*, 2016, **43**, 8306–8313.